CrossMark

ORIGINAL ARTICLE

Expression of glycine receptor alpha 3 in the rat trigeminal neurons and central boutons in the brainstem

Jin Young Bae[1] · Won Mah[1] · Jong-Cheol Rah[2] · Sook Kyung Park[1] · Yong Chul Bae[1]

Abstract Increasing evidence shows that the homomeric glycine receptor is expressed in axon terminals and is involved in the presynaptic modulation of transmitter release. However, little is known about the expression of the glycine receptor, implicated in the presynaptic modulation of sensory transmission in the primary somatosensory neurons and their central boutons. To address this, we investigated the expression of glycine receptor subunit alpha 3 (GlyRα3) in the neurons in the trigeminal ganglion and axon terminals in the 1st relay nucleus of the brainstem by light- and electron-microscopic immunohistochemistry. Trigeminal primary sensory neurons were GlyRα3-immunopositive/gephyrin-immunonegative (indicating homomeric GlyR), whereas GlyRα3/gephyrin immunoreactivity (indicating heteromeric GlyR) was observed in dendrites. GlyRα3 immunoreactivity was also found in the central boutons of primary afferents but far from the presynaptic site and in dendrites at subsynaptic sites. Boutons expressing GlyRα3 contained small round vesicles, formed asymmetric synapses with dendrites and were immunoreactive for glutamate. These findings suggest that trigeminal primary afferent boutons receive presynaptic modulation via homomeric, extrasynaptic GlyRα3, and that different subtypes of GlyR may be involved in pre- and postsynaptic inhibition.

Abbreviations

GlyRα3	Glycine receptor subunit alpha 3
P-ending	Pleomorphic vesicles-containing ending
GABA	γ-Aminobutyric acid
Gly	Glycine
GlyR	Glycine receptor
LM	Light microscopy
EM	Electron microscopy
TG	Trigeminal ganglion
Vp	Trigeminal principal nucleus
DAB	3,3′-Diaminobenzidine
IR	Immunoreactivity

Introduction

The axoaxonic synapses, established by pleomorphic vesicles-containing endings (p-endings) onto primary sensory afferent terminals in the spinal cord and brainstem, are considered the morphological substrate of primary afferent depolarization and presynaptic inhibition (Gray 1962; Alvarez 1998). That presynaptic inhibition is mediated by γ-aminobutyric acid (GABA) and/or glycine (Gly) is suggested by the expression of these neurotransmitters by the presynaptic p-endings (Bae et al. 2000; Watson 2004; Bae et al. 2005b; Moon et al. 2008). The role of GABA in the presynaptic inhibition is confirmed with electrophysiology, and further corroborated by the expression of GABA$_A$ receptor in primary afferents (Désarmenien et al. 1984;

✉ Yong Chul Bae
ycbae@knu.ac.kr

1 Department of Anatomy and Neurobiology, School of Dentistry, Kyungpook National University, 188-1, 2-Ga, Samdeok-Dong, Jung-Gu, Daegu 700-412, South Korea

2 Korea Brian Research Institute, 61 Cheomdan-ro, Dong-gu, Daegu 701-300, South Korea

Labrakakis et al. 2003; Witschi et al. 2011; Lorenzo et al. 2014). However, the role of Gly in presynaptic modulation is made uncertain by the lack of conclusive evidence for the glycine receptor (GlyR) in presynaptic axon terminals (Mitchell et al. 1993; Todd et al. 1996; Lorenzo et al. 2014).

Functional glycine receptors comprise the heteromeric GlyR, composed of α and β subunits, associated with the anchoring protein gephyrin, and the homomeric GlyR, composed of only α subunits (Lynch 2009). Recent studies in many brain regions including neural circuits involved in osmoregulation and auditory processing showed that homomeric and heteromeric GlyR are expressed in distinct axonal and somatodendritic compartments of neurons (Deleuze et al. 2005; Hruskova et al. 2012): while homomeric GlyR is expressed in presynaptic axon terminals (Turecek and Trussell 2002; Kubota et al. 2010; Hruskova et al. 2012), and can be expressed at non-synaptic sites, heteromeric GlyR is expressed at synaptic sites (Mitchell et al. 1993; Todd et al. 1996; Deleuze et al. 2005; Trojanova et al. 2014; Lorenzo et al. 2014).

Aside from some recent reports that the GlyR subunit GlyRα3 is selectively involved in the processing of somatosensory information (Harvey et al. 2004; Lynch 2009), little is known about the expression of GlyR in primary sensory neurons and their central boutons. Here, we report for the first time the expression of GlyRα3, not associated with gephyrin, in the trigeminal primary sensory neurons, suggesting a novel presynaptic modulation of the somatosensory primary afferents via extrasynaptic homomeric GlyR.

Materials and methods

Animals and tissue preparation

Ten male Sprague–Dawley rats, weighing 290–310 g, were used for this study, including four for light microscopic (LM) immunohistochemistry, three for electron microscopic (EM) preembedding immunohistochemistry, and three for EM postembedding immunohistochemistry. All animal procedures were reviewed and approved by the Kyungpook National University Intramural Animal Care and Use Committee.

The rats were deeply anesthetized with sodium pentobarbital (80 mg/kg, i.p.) and perfused intracardially with 100 ml of heparinized normal saline (4000 IU heparin/liter, 0.9 % NaCl solution), followed by 500 ml of freshly prepared fixative. For light microscopy, fixative was 4 % paraformaldehyde in 0.1 M phosphate buffer, pH 7.4 (PB),

for preembedding immunohistochemistry, it was a mixture of 4 % paraformaldehyde and 0.01 % glutaraldehyde in PB, and for postembedding immunohistochemistry, it was a mixture of 4 % paraformaldehyde and 0.5 % glutaraldehyde in PB. The trigeminal ganglion (TG), the dorsal part of its sensory root (to exclude the motor fibers in the ventral root which, separated from the sensory root, passes beneath the TG), and the brainstem, including trigeminal principal (Vp) and caudal (Vc) nuclei, were dissected. The specimens were postfixed in the same fixative for 2 h at 4 °C, and cryoprotected in 30 % sucrose in PB. Sections were cut on a freezing microtome at 40 μm for LM or on a Vibratome at 60 μm for EM, and then stored in PB at 4 °C.

LM immunohistochemistry

For LM immunoperoxidase staining, sections of TG and brainstem, including Vp, were permeabilized with 50 % ethanol for 30 min, blocked with 10 % normal donkey serum (NDS; Jackson ImmunoResearch, West Groove, PA) for 30 min, and incubated overnight in primary antibodies in phosphate buffered saline (PBS; 0.01 M, pH 7.4): rabbit anti-GlyRα3 antibody (1:100; Alomone Labs Ltd., Jerusalem, Israel), goat anti-GlyRα3 (1:100; Santa Cruz Biotechnology, Santa Cruz, CA, USA) and mouse anti-gephyrin antibody (1:300; Synaptic Systems, Göttingen, Germany). After several rinses with PBS and incubation with 2 % NDS for 10 min, sections were incubated with biotinylated donkey anti-rabbit, donkey anti-goat or donkey anti-mouse antibodies (1:200 in PBS; Jackson ImmunoResearch), rinsed in PBS, and incubated with ExtrAvidin peroxidase (1:5000 in PBS; Sigma-Aldrich, St. Louis, MO). Immunoperoxidase was visualized by nickel-intensified 3,3′-diaminobenzidine (DAB), and sections were then lightly counterstained with 1 % thionin. Light micrographs were obtained with an Ex*i* digital camera (Q-imaging Inc., Surrey, CA) attached to a Zeiss Axioplan 2 microscope (Carl Zeiss, Göttingen, Germany), and saved as TIFF files. Size analysis of TG neurons was performed on sections immunostained with rabbit anti-GlyRα3 antibody: The cross-sectional areas of a total of 880 GlyRα3-immunopositive (+) and 848 GlyRα3-immunonegative (−) neurons with clearly visible nucleoli in the opthalmomaxillary and mandibular areas of the TG in 15 sections from the three TGs were measured in micrographs at 400× original magnification using Image J software (http://imagej.nih.gov/ij/, RRID: nif-0000-30467, NIH, Bethesda, MD, USA). Inter-animal variability in the cross-sectional area of somata was not significant (one-way ANOVA, $p = 0.229$), and the data could be pooled for analysis.

EM preembedding immunohistochemistry

For EM, sections of brainstem, including Vp, Vc and dorsal part of sensory root of the TG, were frozen on dry ice for 20 min, thawed in PBS to enhance penetration, and pretreated with 1 % sodium borohydride for 30 min to remove glutaraldehyde. Sections were then blocked with 3 % hydrogen peroxide for 10 min, to suppress endogenous peroxidase, and with 10 % normal donkey serum (NDS) for 30 min, to quench secondary antibody binding sites. Sections were incubated in each primary antibody in PBS overnight at 4 °C: rabbit anti-GlyRα3 (1:50; Alomone Labs Ltd.), goat anti-GlyRα3 (1:50; Santa Cruz Biotechnology) and mouse anti-gephyrin (1:100; Synaptic Systems). For immunoperoxidase staining, the sections were then rinsed in PBS for 15 min, incubated with 2 % NDS for 10 min, and incubated for 2 h in the biotinylated secondary antibody (donkey anti-rabbit, donkey anti-goat or donkey anti-mouse, 1:200; Jackson ImmunoResearch). After rinsing, sections were incubated with ExtrAvidin peroxidase (1:5000; Sigma-Aldrich) for 1 h and the immunoperoxidase was visualized with DAB. Sections were further rinsed in PB, osmicated in osmium tetroxide in PB (1 % for preembedding immunocytochemistry; 0.5 % for postembedding immunocytochemistry) for 1 h. Sections were further dehydrated in graded alcohols, flat-embedded in Durcupan ACM (Fluka, Buchs, Switzerland) between strips of Aclar plastic film (EMS, Hatfield, PA), and cured for 48 h at 58.5 °C. Small pieces containing immunostaining for GlyRα3 or gephyrin in the Vp, Vc and dorsal part of sensory root were cut out of wafers and glued onto blank resin blocks with cyanoacrylate. Thin sections were cut with a diamond knife, mounted on formvar-coated single slot nickel grids, and stained with uranyl acetate and lead citrate. Grids were examined on a Hitachi H 7500 electron microscope (Hitachi, Tokyo, Japan) at 80 kV accelerating voltage. Images were captured with Digital Micrograph software driving a cooled CCD camera (SC1000; Gatan, Pleasanton, CA) attached to the microscope, and saved as TIFF files.

The size of GlyRα3+ axons was analyzed on sections immunostained with the rabbit anti-GlyRα3 antibody: The cross-sectional areas of a total of 560 GlyRα3+ axons and the thickness of their myelin sheath were measured in micrographs at 10,000× or 25,000× original magnification from nine sections of the dorsal part of the trigeminal sensory root in three TGs using Image J (v 1.6, NIH, Bethesda, MD). Correlation analysis with Fisher's r-to-z transformation for significance was used to test relationships between the cross-sectional area of the myelinated axons and the thickness of their myelin sheath. Significance was set at $p < 0.05$. Inter-animal variability in the proportion of each fiber type within the same group was insignificant (Pearson Chi square test, $p = 0.125$), and the data could be pooled per group for analysis. Immunopositive fibers were grouped into unmyelinated, small myelinated ($<20\ \mu m^2$ cross-sectional area, equivalent to $<5\ \mu m$ in diameter), and large myelinated fibers ($>20\ \mu m^2$ cross-sectional area, equivalent to $>5\ \mu m$ in diameter), corresponding to C, Aδ and Aα/β fibers, respectively, according to previous studies which emphasized the correlation between conduction velocity and axonal diameter in myelinated axons (Debanne et al. 2011; Boron and Boulpaep 2012).

We further analyzed the expression of GlyRα3 in the boutons and dendrites in the Vp and Vc. We focused on the Vp, because of its highest frequency of axoaxonic synapses, associated with trigeminal primary sensory afferents, among the trigeminal sensory nuclei, and because of its dense input of peptidergic and non-peptidergic C afferents, mechanoreceptive Aβ afferents, and mainly Aδ, pulpal afferents (Bae et al. 1994; Sugimoto et al. 1997a, b; Bae et al. 2003).

EM postembedding immunogold staining

Multiple sets of 3–4 serial sections from each resin block containing sections performed with immunoperoxidase staining for GlyRα3 were used for immunogold staining for glutamate and glycine. Immunogold labeling was performed as previously published by our laboratory (Bae et al. 2002; Paik et al. 2007). Briefly, the grids were treated in 1 % periodic acid for 10 min, to etch the resin, in 9 % sodium periodate for 15 min, to remove the osmium tetroxide, then washed in distilled water, transferred to tris-buffered saline containing 0.1 % triton X-100 (TBST; pH 7.4) for 10 min, and incubated in 2 % human serum albumin (HSA) in TBST for 10 min, to block non-specific binding of primary antibodies. The grids were then incubated with rabbit polyclonal antisera against glutamate (Glut 607, 1:1000) and glycine (Gly 290, 1:280) in TBST containing 2 % HSA for 2 h at room temperature. To eliminate cross-reactivity, the diluted antisera were preadsorbed overnight with glutaraldehyde (G)-conjugated amino acids (300 μM glutamine-G, 100 μM aspartate-G, and 200 μM β-alanine-G for glutamate, 300 μM β-alanine-G and 200 μM GABA-G for glycine, Ottersen et al. 1986). After extensive rinsing in TBST, grids were incubated for 3 h in goat anti-rabbit IgG coupled to 15 nm gold particles (1:25 in TBST containing 0.05 % polyethylene glycol; BioCell, Cardiff, UK). After a rinse in distilled water, the grids were counterstained with uranyl acetate and lead citrate and examined and images were captured as above.

To assess the immunoreactivity for glutamate, gold particle density (number of gold particles per μm^2) over each GlyRα3+ bouton was compared to the average tissue density
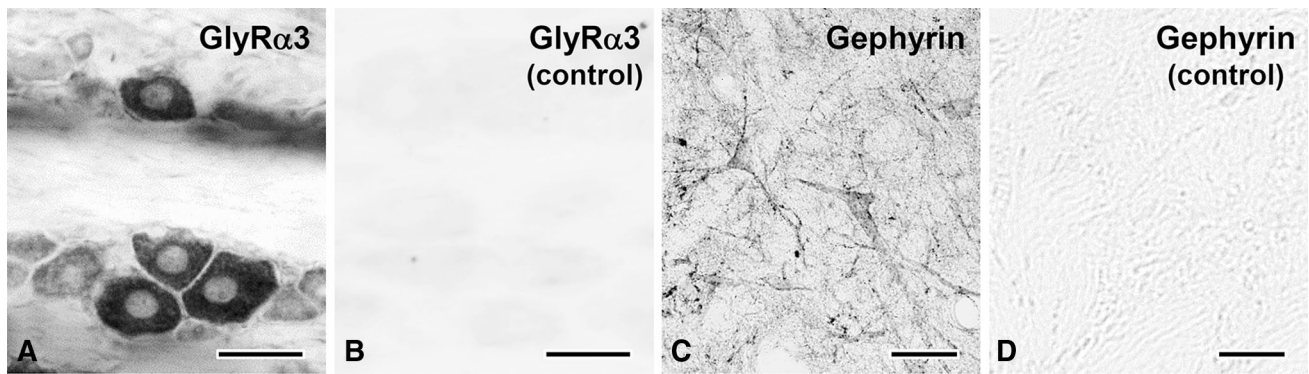
Fig. 1 Light micrographs showing specificity of immunostaining for GlyRα3 (a, b) and gephyrin (c, d) in the trigeminal ganglion (TG; a, b) and trigeminal principal nucleus (Vp; c, d). Immunostaining was completely abolished by preadsorption with the corresponding blocking peptide (10 μg/ml: b), or by omission of the primary antibody (d). Scale bars 50 μm

in 5–10 randomly-selected areas adjacent to the GlyRα3+ bouton (2 μm^2 each, a total area of 10–20 μm^2 per section). Boutons containing gold particles at a density >2.576 SD of the average tissue density (99 % confidence level) were considered glutamate-immunopositive (Shigenaga et al. 2005; Paik et al. 2011, 2012a). To assess the immunoreactivity for glycine, gold particle density of the p-endings forming axoaxonic synapses with GlyRα3+ boutons and that of the axon terminal forming axodendritic synapses with GlyRα3+ dendrites was compared with the gold particle density of presumed excitatory boutons containing round vesicles and forming asymmetrical synaptic contact with dendrites. P-endings forming axoaxonic synapses or axon terminals forming axodendritic synapses were considered glycine-immunopositive if the gold particle density for glycine over the vesicle-containing areas was at least five times higher than that in the excitatory boutons.

Antibodies and immunohistochemical controls

The antibody against GlyRα3 (Alomone Labs Ltd., Cat. No. AGR-003, lot AN-01) is a polyclonal antibody raised against a peptide corresponding to amino acids 355–368 (KNKTEAFALEKFYR) of the second intracellular loop of rat GlyRα3. We performed a Blast search against the NCBI's GenBank and found that the antigen is homologous to GlyRα3, and not to any other peptide in the database. The antibody against gephyrin (Synaptic Systems, Cat. No. 147-021, clone mAb7a, lot 147021/15) is a monoclonal antibody raised against the N-terminus of gephyrin, surrounding phospho-serines 268 and 270. It has been extensively characterized in previous studies (Kneussel et al. 1999; Javdani et al. 2015; Fekete et al. 2015).

To test the specificity of the rabbit anti-GlyRα3 and mouse anti-gephyrin antibodies in sections of TG and Vp, (1) we performed preadsorption with the immunizing peptide (GlyRα3: Alomone Labs Ltd., AG-01): 10 μg of anti-GlyRα3 antibody was incubated with 1, 5 or 10 μg/ml of the immunizing peptide for 2 h at room temperature, centrifuged at 15,000 rpm for 10 min, and the supernatant was used for preadsorption. Preadsorption with 1 or 5 μg/ml of the immunizing peptide reduced the GlyRα3-immunoreactivity, and preadsorption with 10 μg/ml completely abolished it (Fig. 1). (2) We compared the expression pattern of GlyRα3 in TG neurons, sensory root of the TG, and boutons and dendrites in Vp, in sections immunostained with rabbit anti-GlyRα3 antibody (Alomone) to that in sections immunostained with goat anti-GlyRα3 antibody (Santa Cruz Biotechnology), which was extensively characterized, using GlyRα3$^{-/-}$ mice (Haverkamp et al. 2003). The expression pattern with the two antibodies was identical. (3) We processed sections according to the same immunostaining protocols, except that the primary or secondary antisera were omitted or replaced by normal serum. Omission or substitution of the antisera completely abolished the immunostaining. (4) The specificity of immunostaining was also confirmed by the consistency of immunostaining in the same boutons or dendrites in adjacent serial thin sections.

The rabbit polyclonal antisera against glutamate (Glut 607, 1:1000) and glycine (Gly 290, 1:280), a gift from Dr. Ole P. Ottersen at the University of Oslo, have been used routinely in our previous works (Bae et al. 2000, 2002; Paik et al. 2012b). They were raised according to the procedure of Storm-Mathisen et al. (1983), except that the amino acids were conjugated to bovine serum albumin by glutaraldehyde and formaldehyde instead of glutaraldehyde alone, and extensively characterized (Broman et al. 1993; Matsubara et al. 1996; Takumi et al. 1999). Their specificity was confirmed on test sections of 'sandwiches' of rat brain macromolecule-glutaraldehyde complexes of different amino acids, including GABA, glycine, and glutamate (Zhang and Ottersen 1992; Bae et al. 2000; Paik et al. 2012b). Test sections were incubated in the same drops of

glutamate and glycine antisera as the tissue sections, and the respective conjugates in the test sections were selectively labeled. Furthermore, omission or replacement of the primary antisera with normal rabbit serum or preadsorption of the diluted anti-glutamate serum with 300 μM Glut-G and anti-glycine serum with 300 μM Gly-G abolished the specific immunostaining, confirming the selectivity of the antisera.

Results

At LM, the immunoperoxidase staining for GlyRα3 in TG was observed in neurons of all sizes. In contrast, TG neurons were negative for gephyrin (Fig. 2). Immunoreactivity (IR) of GlyRα3 and gephyrin was completely abolished by preadsorption with the corresponding blocking peptide or by omission of the primary antibody

Fig. 2 Light micrographs showing immunoperoxidase staining for GlyRα3 (a with a rabbit anti-GlyRα3 antibody; b with a goat anti-GlyRα3 antibody) and gephyrin (c) in the TG, and size distribution of GlyRα3+ neurons (d). TG neurons of all sizes are immunostained for GlyRα3, but not for gephyrin. Scale bar 50 μm

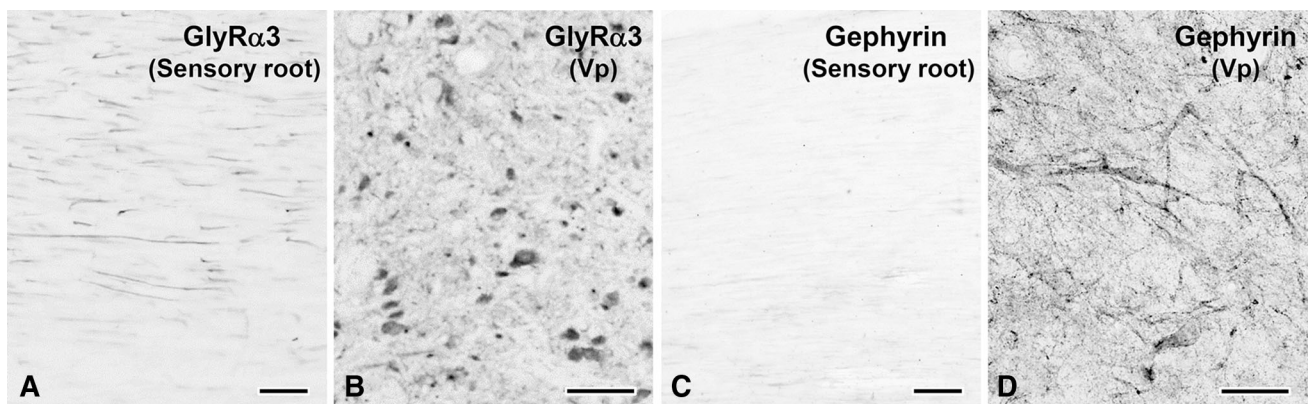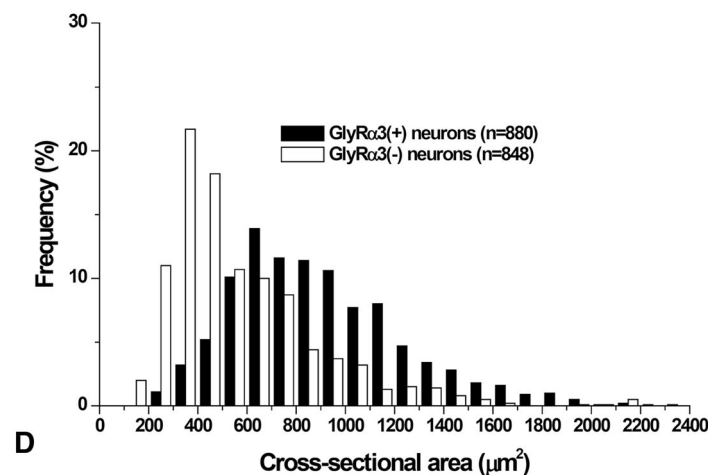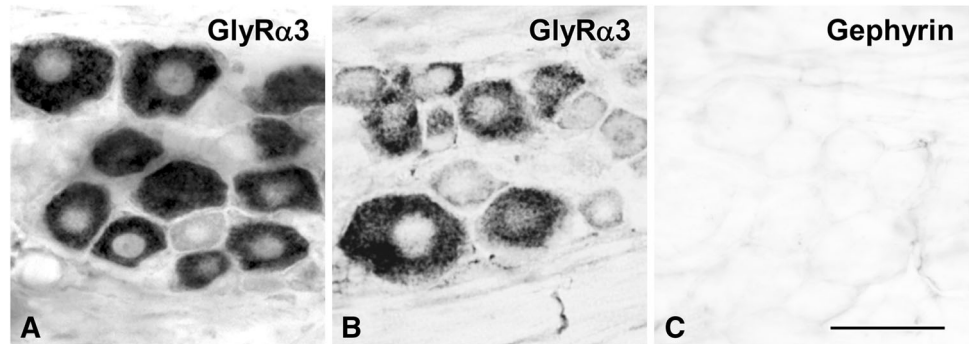Fig. 3 Light micrographs showing immunoperoxidase staining for GlyRα3 (a, b) and gephyrin (c, d) in the sensory root of the trigeminal ganglion (a, c) and trigeminal principal nucleus (Vp: b, d). GlyRα3-immunoreactivity (IR) is observed in nerve fibers in the sensory root and in Vp, whereas gephyrin-IR is observed in the Vp, but not in the sensory root. Scale bars 50 μm
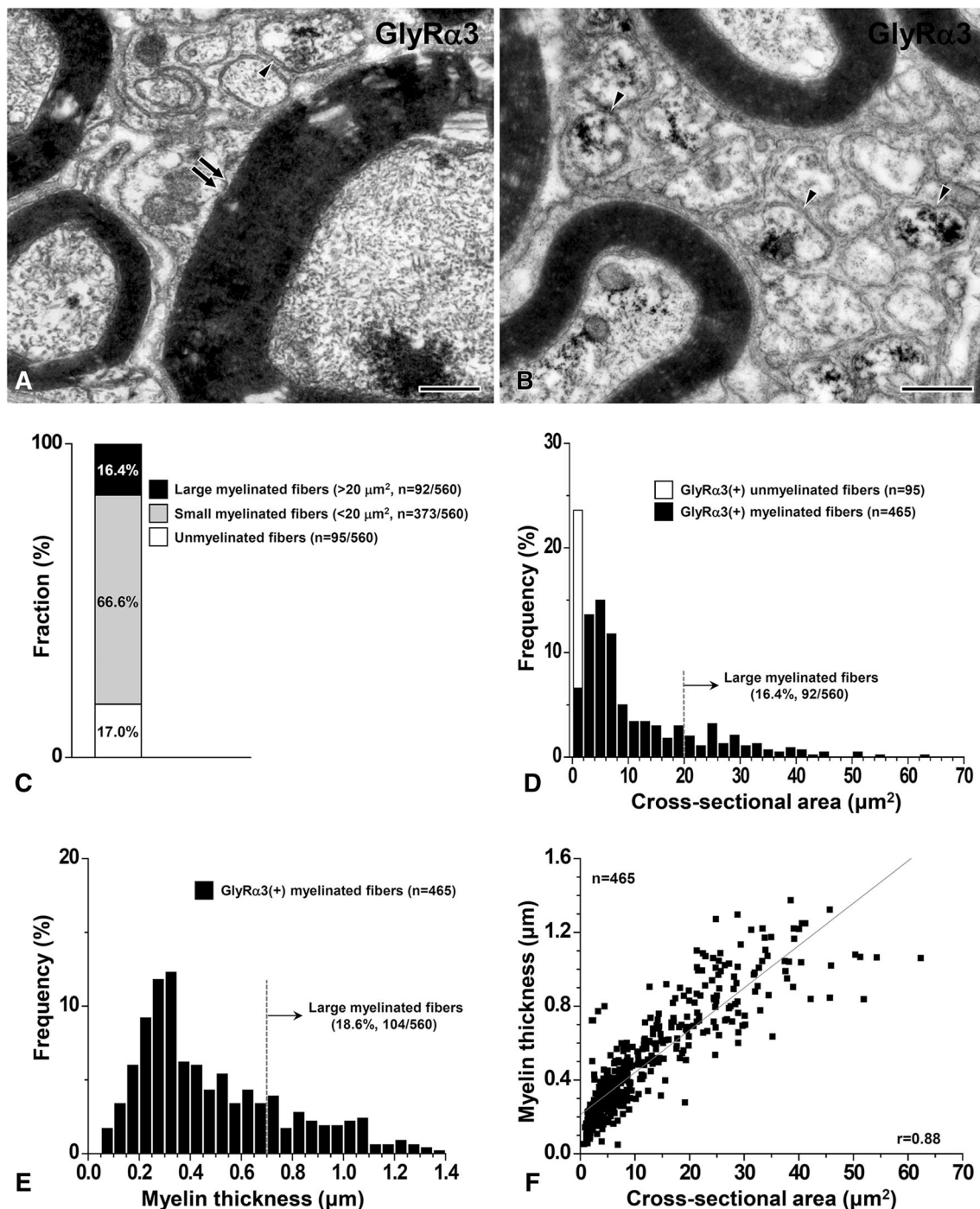
Fig. 4 GlyRα3-positive (+) fibers in the sensory root of the trigeminal ganglion. **a**, **b** Electron micrographs showing GlyRα3+ - large myelinated (*double arrows*) and unmyelinated (*arrowhead*) fibers. **c**, **d** *Stacked histograms* showing the fraction (**c**) and size distribution (**d**) of the GlyRα3+ unmyelinated, small myelinated, and large myelinated fibers. Most GlyRα3+ fibers are small myelinated (∼67 %: <20 μm^2 in cross-sectional area, equivalent to <5 μm in diameter, *left* to the *dotted line*) and unmyelinated (17 %). **e** Histogram showing the thickness of myelin sheath of the GlyRα3+ myelinated fibers. The average thickness of the myelin sheath of GlyRα3+ fibers with ∼20 μm^2 cross-sectional area is 0.7 μm. **f** Correlation between the thickness of the myelin sheath and the cross-sectional area of the GlyRα3+ myelinated fibers. *r* correlation coefficient. *Scale bars* 500 nm

(Fig. 1b, d). GlyRα3- IR was also observed both in the sensory root of the TG and Vp, whereas gephyrin-IR was observed in the Vp but not in the sensory root (Fig. 3).

At EM, electron-dense immunoreaction product, coding for GlyRα3, seemed to be associated with microtubules and sometimes spread into the adjacent axoplasm, but remained

within the axons. GlyRα3-immunoreactivity (IR) was observed mostly in small myelinated (<20 μm² in cross-sectional area, equivalent to <5 μm in diameter, corresponding to Aδ fibers: 66.6 %), but also large myelinated (>20 μm² in cross-sectional area, corresponding to Aβ fibers: 16.4 %), and unmyelinated (17.0 %, Fig. 4). We also classified the myelinated fibers, based on the thickness on their myelin with a cutoff thickness of 0.7 μm, which was the average myelin thickness of myelinated fibers with cross-sectional area of 20 μm². The fractions of small (<0.7 μm in myelin thickness, 64.5 %) and large (>0.7 μm, 18.6 %) were similar to those classified based on cross-sectional area. In addition, the cross-sectional area of the GlyRα3+ myelinated fibers was positively corre-

lated with their myelin thickness (Fig. 4e, f). Gephyrin-immunopositive (+) fibers were not observed.

In the Vp, the trigeminal principal nucleus in the brainstem, the immunostaining for GlyRα3 was in boutons, some receiving axoaxonic synapses, and some not (Fig. 5). GlyRα3-immunoreactivity (IR) was also observed in dendrites receiving synapses from axon terminals containing round, oval and/or flattened vesicles (Fig. 6). Gephyrin-IR was not observed in boutons (Fig. 7a, b), suggesting homomeric GlyR expression in boutons, however, both GlyRα3-IR and gephyrin-IR were observed in dendrites, suggesting heteromeric GlyR expression in dendrites (Figs. 6a, b, 7c, d). The expression pattern of GlyRα3 in the boutons and dendrites in the Vc was similar to that in the Vp.

Fig. 5 Electron micrographs of GlyRα3-immunopositive (+) boutons (*asterisks*), which receive axoaxonic synaptic contacts from endings that contain pleomorphic vesicles (*p1, p2*) and form glomeruli with multiple postsynaptic dendrites (**a** *d1–d4*), or contact single dendrites (**b–d** *d*) in the trigeminal principal nucleus. GlyRα3-immunoreactivity (*arrows*) is localized near the plasma membrane away from the synapses. Note that GlyRα3+ boutons contain round vesicles. The GlyRα3+ boutons and p-endings are outlined with a *dashed line*, *arrowheads* indicate synapses. *Scale bars* 500 nm
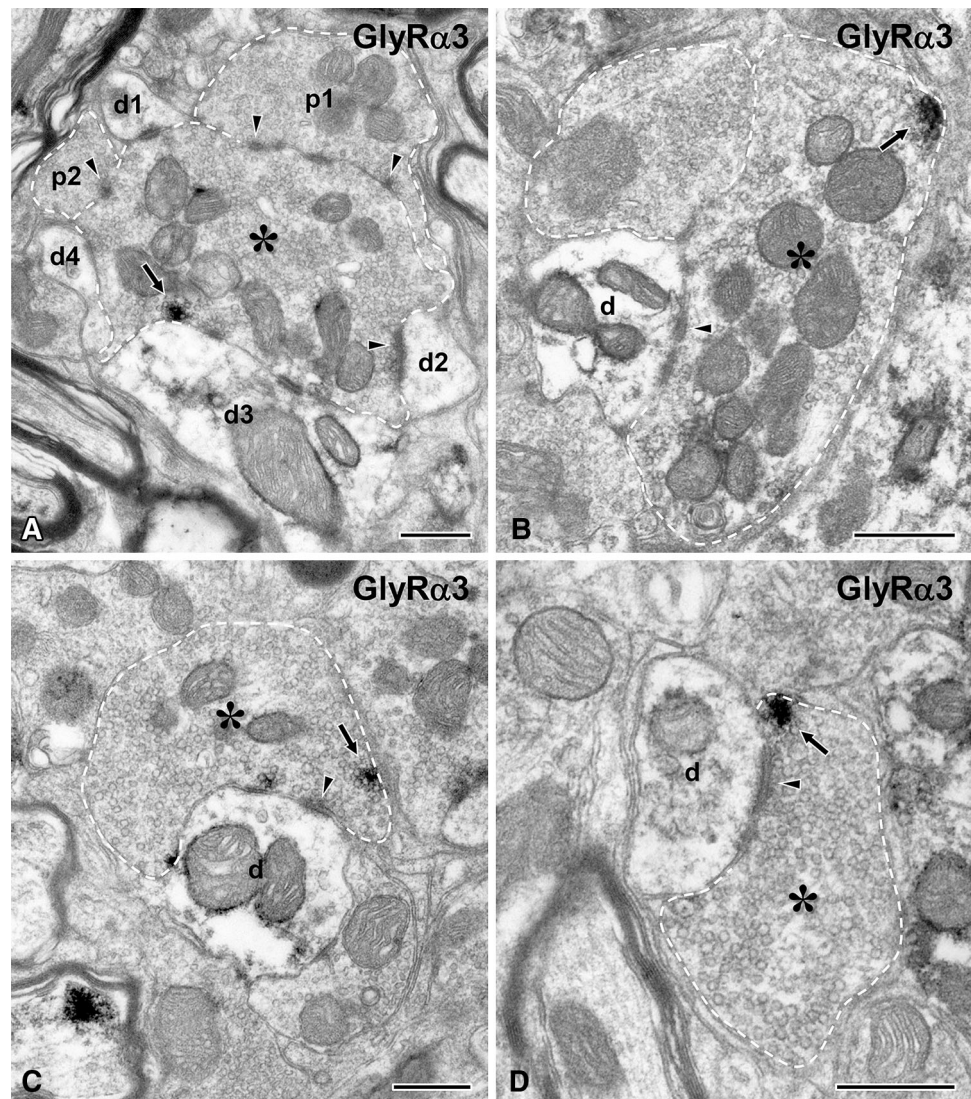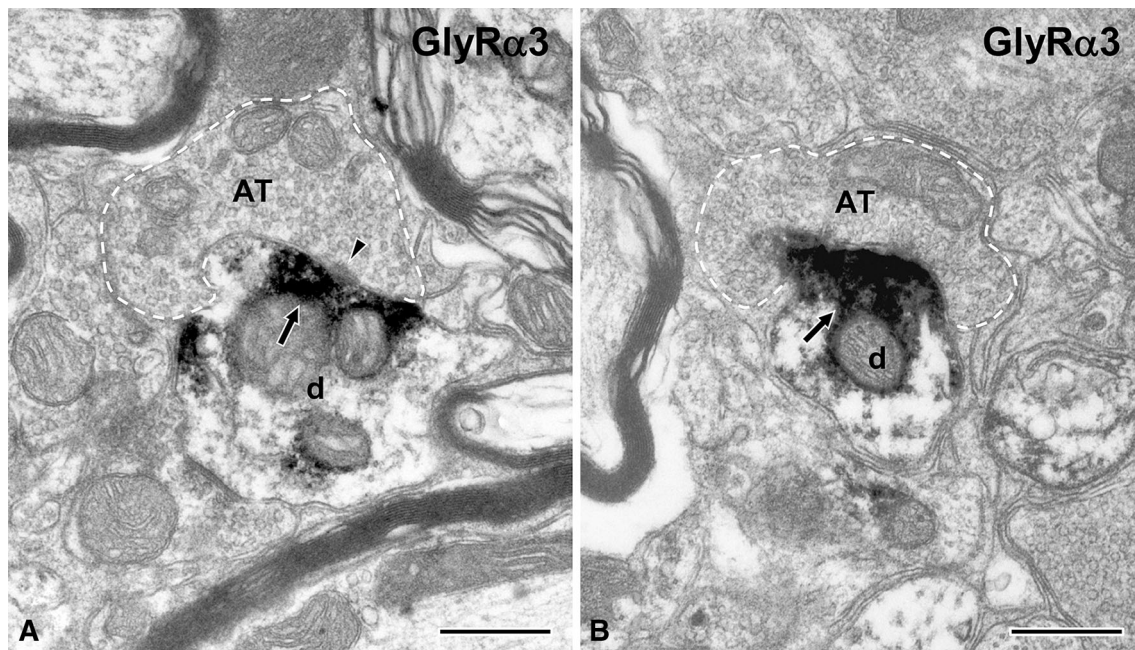
Fig. 6 Electron micrographs of GlyRα3-immunopositive (+) dendrites (*d*) that receive synaptic contacts from axon terminals (*AT*) in the trigeminal principal nucleus. GlyRα3-immunoreactivity (*arrows*) is localized to the subsynaptic area. The axon terminals are outlined with a *dashed line*, *arrowhead* indicates synapse. *Scale bars* 500 nm

The immunostaining for GlyRα3 in boutons was in the form of small patches near the plasma membrane away from synapses, whereas in dendrites, both GlyRα3-IR and gephyrin-IR were clustered at the subsynaptic zone. The GlyRα3+ boutons contained small clear round vesicles, made asymmetric synaptic contacts with dendrites, and immunostained for glutamate, suggesting that they are excitatory (Fig. 8a, b). They frequently received axoaxonic synapses from small presynaptic endings, which contained pleomorphic vesicles, and immunostained for glycine (Fig. 8c, d). The axon terminals forming symmetric synapses with GlyRα3+/gephyrin+ dendrites were also glycine+ (Fig. 8e, f).

Discussion

The main findings of the present study are that (1) GlyRα3, but not gephyrin, is expressed in trigeminal primary sensory neurons and their central boutons, whereas GlyRα3 and gephyrin are co-expressed in dendrites in the brainstem, and (2) GlyRα3 is localized away from the synapse in boutons and at subsynaptic sites in dendrites. These findings provide a morphological support for the notion that primary somatosensory afferent boutons receive glycine-mediated presynaptic modulation via extrasynaptic, homomeric GlyRα3. They also suggest that different subtypes of GlyR (homomeric vs. heteromeric) mediate the pre- and postsynaptic glycinergic inhibition.

Expression of GlyRα3, but not gephyrin, in the primary sensory neurons and central boutons

Consistent with previous studies in the spinal cord (Mitchell et al. 1993; Todd et al. 1995; Lorenzo et al. 2014), gephyrin-IR was not observed in the central boutons. However, GlyRα3-IR was observed in the primary sensory neurons and central boutons, suggesting that they express homomeric GlyR. Homomeric GlyR has also been shown in axon terminals in the hippocampus, the auditory nucleus, and the supraoptic nucleus (Sassoe-Pognetto et al. 1994; Turecek and Trussell 2001, 2002; Deleuze et al. 2005; Kubota et al. 2010). Conversely, dendrites were immunostained for both GlyRα3 and gephyrin, indicating that they express heteromeric GlyR and suggesting that while homomeric GlyRα3 may be involved in presynaptic modulation in boutons, heteromeric GlyRα3 may be involved in postsynaptic inhibition in dendrites. This supports the electrophysiological observations of large glycine-gated channel conductance, consistent with homomeric GlyR, in the presynaptic terminals, but small channel conductance, consistent with heteromeric GlyR, in the somatodendritic compartment of spinal- and brainstem neurons (Takahashi et al. 1992; Turecek and Trussell 2002; Beato and Sivilotti 2007; Lynch 2009). It is also consistent with studies of the hypothalamic and auditory neurons, showing differential distribution of homomeric and heteromeric GlyR in the axonal and

Fig. 7 Electron micrographs of boutons (**a, b**) and dendrites (**c, d**) immunostained for gephyrin in the trigeminal principal nucleus. **a, b** Gephyrin immunoreactivity is not observed in boutons (*asterisk*) containing round vesicles and/or forming asymmetrical synaptic contacts with dendrites (*d*). **c, d** Gephyrin-immunoreactivity (*arrows*) is localized to the subsynaptic area of dendrites (*d*), which receive synapses from axon terminals (*AT*), containing a mixture of round, oval, and flattened vesicles. Axon terminals are outlined with a *dashed line*, *arrowheads* indicate synapses. *Scale bars* 500 nm
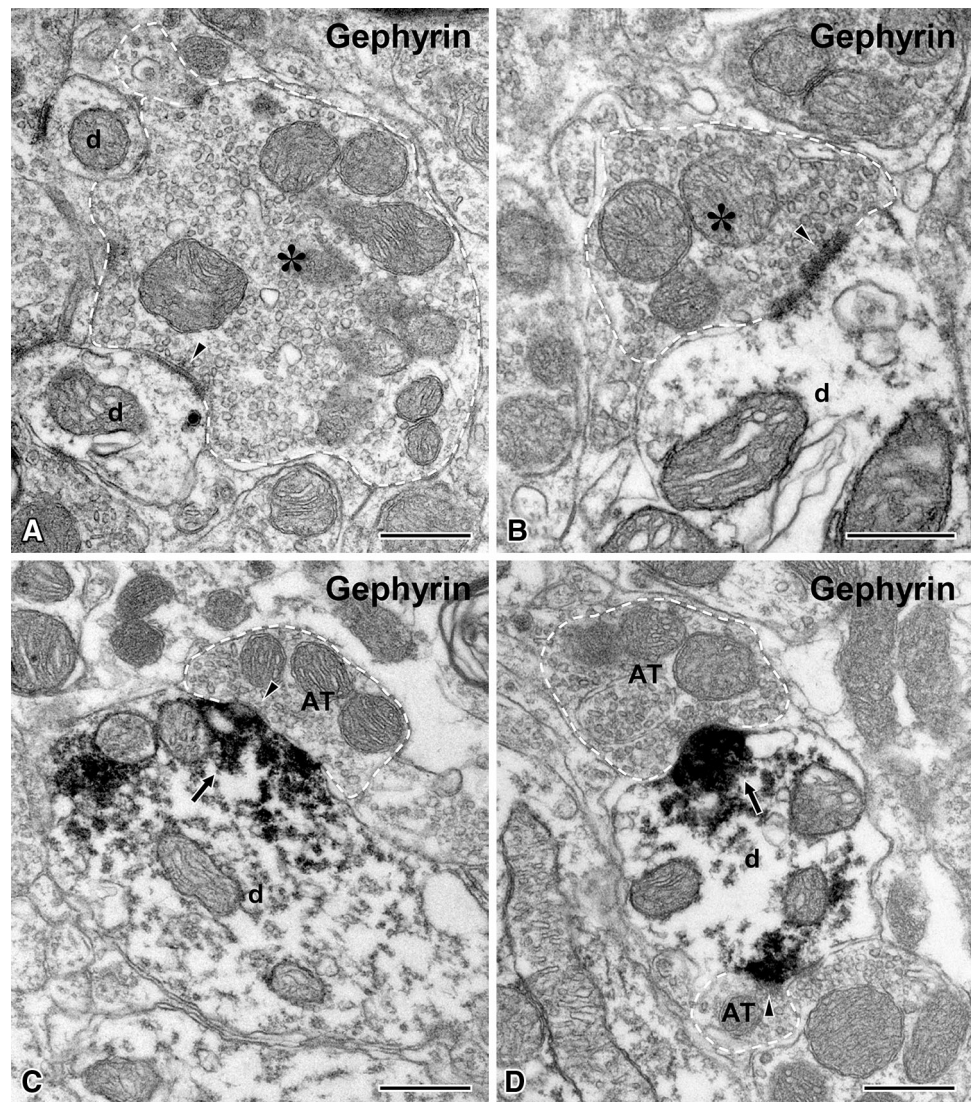

somatodendritic compartments, respectively (Deleuze et al. 2005; Hruskova et al. 2012).

In the present study, the GlyRα3+ boutons contained clear round vesicles, formed asymmetrical synaptic contacts with dendrites, and were immunostained for glutamate, suggesting that they are excitatory. In addition, they usually established synaptic contacts with multiple dendrites and axonal endings, and formed glomeruli, analogous to the A and C afferent terminals in the spinal dorsal horn (Ribeiro-da-Silva and Coimbra 1982; Alvarez et al. 1992) and trigeminal sensory nuclei (Bae et al. 1994, 2005a). In addition, a previous study showed that the axon terminals of excitatory local circuit neurons in the brainstem are rarely involved in axoaxonic synapses (Paik et al. 2009). Considering these present and previous findings, we assumed that most GlyRα3+ central boutons are of primary afferent origin.

In the present study, the fraction of small-sized GlyRα3+ somata was 4 %, but that of unmyelinated axons was 17 %. Also, only 44 % of the GlyRα3+ somata were small- and medium-sized, but 84 % of the GlyRα3+ axons were unmyelinated or small myelinated. This suggests that large GlyRα3+ somata may have small axons. This is supported by a recent study in TG, showing that most medium-sized neurons (400–800 μm^2) have unmyelinated axons, and that while only a third of the CGRP+ somata are medium- or large-sized (>400 μm^2), 97 % of the CGRP+ axons are unmyelinated (Bae et al. 2015).

In contrast with the size distribution of dorsal root ganglion neurons, which has one peak for the small, and one peak for the large neurons (Harper and Lawson 1985), the TG neurons had a single peak of size distribution (Wotherspoon and Priestley 1999; Ichikawa et al. 2003; Triner 2013), the low fraction of large cells being

Fig. 8 Electron micrographs of adjacent thin sections of the trigeminal principal nucleus, simultaneously stained for GlyRα3 with immunoperoxidase, and with immunogold for glutamate (**a**, **b**) or glycine (**c**–**f**). **a**, **b** A GlyRα3+ bouton (*asterisk*) containing round vesicles and forming synapses with dendrites (*d1*, *d2*), is glutamate-immunopositive. **c**, d A GlyRα3+ bouton (*asterisk*) receives a synapse from a glycine+ presynaptic ending (*p*), and establishes a synaptic contact with a dendrite (*d*). **e**, **f** A GlyRα3+ dendrite receives a synapse from a glycine+ axon terminal (*AT*). Axon terminals are outlined with a *dashed line*, *arrows* indicate immunostaining for GlyRα3, *arrowheads* indicate synapses. *Scale bars* 500 nm
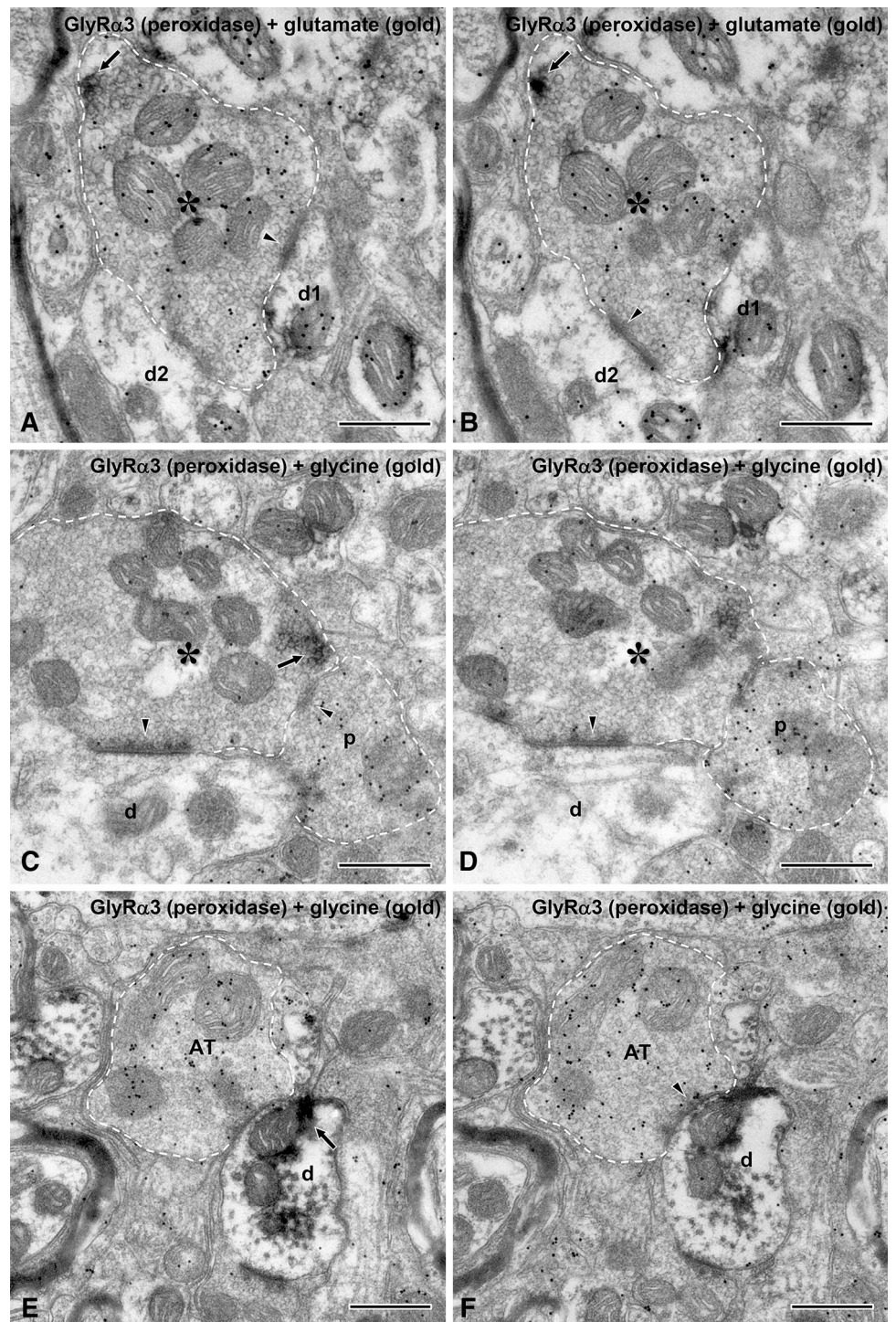
presumably due to the lack of large proprioceptive neurons in the TG (Shigenaga et al. 1988).

Extrasynaptic GlyRα3 on the central boutons

It has been shown before in many brain regions that functional homomeric GlyR in axon terminals such as calyx terminals is localized to extrasynaptic sites, which are involved in the modulation of glutamate release (Turecek and Trussell 2002; Kubota et al. 2010; Hruskova et al. 2012; Trojanova et al. 2014; Xiong et al. 2014). In the present study, GlyR-IR in boutons was near the plasma membrane away from synaptic sites, and rarely at axoaxonic contacts by p-endings, whereas in dendrites, it was at

synaptic sites, showing that homomeric GlyR is at extrasynaptic sites of boutons, and that heteromeric GlyR is at synaptic sites in dendrites.

The functional properties of receptors expressed on the neuronal cell membrane differ according to their subcellular location. Thus, GlyR expressed at extrasynaptic sites in axon terminals is slowly and tonically activated via paracrine release or spillover of glycine from adjacent glycine+ boutons or non-neuronal cells (Turecek and Trussell 2001; Muller et al. 2008; Kopp-Scheinpflug et al. 2008). The subsequent opening of GlyR induces efflux of Cl^-, due to the high intracellular $[Cl^-]$ in the presynaptic boutons (Kim and Trussell 2009; Chu et al. 2012), causing depolarization and an increase in Ca^{2+} concentration (Turecek and Trussell 2001; Price and Trussell 2006; Huang and Trussell 2008), and subsequent modulation of neurotransmitter release (Chu et al. 2012). In contrast, heteromeric GlyR, clustered at subsynaptic sites of the somatodendritic compartment, are rapidly and transiently activated by glycine released into the synaptic cleft, followed by a rapid clearing from the synapse (Singer and Berger 2000; Legendre 2001; Muller et al. 2008; Hruskova et al. 2012). Therefore, the extrasynaptic GlyRα3 in boutons may be involved in the slow, tonic modulation of glutamate release, whereas the synaptic GlyRα3 in dendrites may be involved in fast, phasic inhibitory response of the postsynaptic neuron.

In the present study, the immunostaining for GlyRα3 in dendrites was dense and covered large irregular territories in the cytoplasm, partly adjacent to the postsynaptic membrane, and partly to the outer membranes of mitochondria. We interpret this to indicate a large amount of GlyRα3 in the subsynaptic area, but we cannot exclude that it may also be caused by an artifactual diffusion of DAB. On the other hand, the GlyRα3-IR in boutons was weak and in the form of small patches, indicating relatively small amounts of GlyRα3. Boutons, compared to dendrites, have smaller size and surface area and thus may have higher input resistance and lower capacitance, so that small ion influxes into a bouton can result in large changes in the membrane potential. Furthermore, homomeric GlyR has larger channel conductance (Bormann et al. 1993; Handford et al. 1996) and slower deactivation and desensitization rates than heteromeric GlyR (Legendre 2002; Mohammadi et al. 2003). Because of that, it is conceivable that small amounts of GlyRα3 can efficiently modulate glutamate release from boutons. Administration of strychnine and L-type Ca^{2+} channel blockers inhibits accumulation of GlyR at the postsynaptic membrane of spinal neurons, suggesting that Ca^{2+} influx may induce accumulation of GlyR at synaptic sites (Levi et al. 1998; Kirsch and Betz 1998). If this is applicable to the GlyRα3+ boutons, activation of a small amount of extrasynaptic GlyR may induce accumulation of GlyR to the extrasynaptic sites,

which in turn, may induce large GlyR-mediated currents that are sufficient for the effective modulation of glutamate release from the bouton.

At present, the source for glycine necessary for the activation of extrasynaptic GlyR in boutons is unknown. One such source may be glycine spillover from the glycine+ p-ending, presynaptic to the GlyRα3+ bouton, or from adjacent glycine+ axon terminals. Another is the paracrine release of glycine (or the glycine receptor agonist taurine) from surrounding astrocytes (Hussy et al. 1997; Kopp-Scheinpflug et al. 2008).

GlyRα3 was expressed in trigeminal neurons of all sizes and in fibers of all types, suggesting a role of GlyRα3 in presynaptic modulation of Aδ- and C-fiber-mediated nociception, as well as Aβ-fiber-mediated mechanoreception. That most GlyRα3+ fibers were unmyelinated and small myelinated suggests a predominant role of GlyRα3 in nociception. This is corroborated by recent reports that inhibition of GlyRα3 by prostaglandin E2-induced receptor phosphorylation, induces central pain sensitization during inflammation (Harvey et al. 2004, 2009). Also, cannabinoids suppress inflammatory pain by selectively potentiating GlyRα3-mediated glycinergic currents (Xiong et al. 2012). These results implicate homomeric GlyRα3 in boutons, as well as heteromeric GlyRα3 in dendrites, in the mechanism of central pain hypersensitivity during inflammation.

References

Alvarez FJ (1998) Anatomical basis of presynaptic inhibition of primary afferent fibers. In: Rudomin P, Romo R, Mendell LM (eds) Presynaptic inhibition and neural control. Oxford University Press, New York, pp 13–49

Alvarez F, Kavookjian A, Light A (1992) Synaptic interactions between GABA-immunoreactive profiles and the terminals of functionally defined myelinated nociceptors in the monkey and cat spinal cord. J Neurosci 12:2901–2917

Bae YC, Nakagawa S, Yoshida A, Nagase Y, Takemura M, Shigenaga Y (1994) Morphology and synaptic connections of slowly adapting periodontal afferent terminals in the trigeminal subnuclei principalis and oralis of the cat. J Comp Neurol 348:121–132

Bae YC, Ihn HJ, Park MJ, Ottersen OP, Moritani M, Yoshida A, Shigenaga Y (2000) Identification of signal substances in synapses made between primary afferents and their associated axon terminals in the rat trigeminal sensory nuclei. J Comp Neurol 418:299–309

Bae YC, Choi BJ, Lee MG, Lee HJ, Park KP, Zhang LF, Honma S, Fukami H, Yoshida A, Ottersen OP, Shigenaga Y (2002) Quantitative ultrastructural analysis of glycine- and gamma-aminobutyric acid-immunoreactive terminals on trigeminal

alpha- and gamma-motoneuron somata in the rat. J Comp Neurol 442:308–319

Bae YC, Kim JP, Choi BJ, Park KP, Choi MK, Moritani M, Yoshida A, Shigenaga Y (2003) Synaptic organization of tooth pulp afferent terminals in the rat trigeminal sensory nuclei. J Comp Neurol 463:13–24

Bae YC, Ahn HJ, Park KP, Kim HN, Paik SK, Bae JY, Lee HW, Kim KH, Yoshida A, Moritani M, Shigenaga Y (2005a) The synaptic microcircuitry associated with primary afferent terminals in the interpolaris and caudalis of trigeminal sensory nuclear complex. Brain Res 1060:118–125

Bae YC, Park KS, Bae JY, Paik SK, Ahn DK, Moritani M, Yoshida A, Shigenaga Y (2005b) GABA and glycine in synaptic microcircuits associated with physiologically characterized primary afferents of cat trigeminal principal nucleus. Exp Brain Res 162:449–457

Bae JY, Kim JH, Cho YS, Mah W, Bae YC (2015) Quantitative analysis of afferents expressing substance P, calcitonin gene-related peptide, isolectin B4, neurofilament 200, and peripherin in the sensory root of the rat trigeminal ganglion. J Comp Neurol 523:126–138

Beato M, Sivilotti LG (2007) Single-channel properties of glycine receptors of juvenile rat spinal motoneurones in vitro. J Physiol 580:497–506

Bormann J, Rundström N, Betz H, Langosch D (1993) Residues within transmembrane segment M2 determine chloride conductance of glycine receptor homo- and hetero-oligomers. EMBO J 12:3729–3737

Boron WF, Boulpaep EL (2012) Medical physiology: a cellular and molecular approach. Saunders/Elsevier, Philadelphia

Broman J, Anderson S, Ottersen OP (1993) Enrichment of glutamate-like immunoreactivity in primary afferent terminals throughout the spinal cord dorsal horn. Eur J Neurosci 5:1050–1061

Chu Y, Fioravante D, Thanawala M, Leitges M, Regehr WG (2012) Calcium-dependent isoforms of protein kinase C mediate glycine-induced synaptic enhancement at the calyx of held. J Neurosci 32:13796–13804

Debanne D, Campanac E, Bialowas A, Carlier E, Alcaraz G (2011) Axon physiology. Physiol Rev 91:555–602

Deleuze C, Runquist M, Orcel H, Rabié A, Dayanithi G, Alonso G, Hussy N (2005) Structural difference between heteromeric somatic and homomeric axonal glycine receptors in the hypothalamo-neurohypophysial system. Neuroscience 135:475–483

Désarmenien M, Feltz P, Occhipinti G, Santangelo F, Schlichter R (1984) Coexistence of GABAA and GABAB receptors on Aδ and C primary afferents. Br J Pharmacol 81:327–333

Fekete CD, Chiou T-T, Miralles CP, Harris RS, Fiondella CG, Loturco JJ, De Blas AL (2015) In vivo clonal overexpression of neuroligin 3 and neuroligin 2 in neurons of the rat cerebral cortex: differential effects on GABAergic synapses and neuronal migration. J Comp Neurol 523:1359–1378

Gray EG (1962) A morphological basis for pre-synaptic inhibition? Nature 193:82–83

Handford CA, Lynch JW, Baker E, Webb GC, Ford JH, Sutherland GR, Schofield PR (1996) The human glycine receptor β subunit: primary structure, functional characterisation and chromosomal localisation of the human and murine genes. Mol Brain Res 35:211–219

Harper AA, Lawson SN (1985) Conduction velocity is related to morphological cell type in rat dorsal root ganglion neurones. J Physiol 359:31–46

Harvey RJ, Depner UB, Wässle H, Ahmadi S, Heindl C, Reinold H, Smart TG, Harvey K, Schütz B, Abo-Salem OM, Zimmer A, Poisbeau P, Welzl H, Wolfer DP, Betz H, Zeilhofer HU, Müller U (2004) GlyR alpha3: an essential target for spinal PGE2-mediated inflammatory pain sensitization. Science 304:884–887

Harvey VL, Caley A, Müller UC, Harvey RJ, Dickenson AH (2009) A selective role for alpha3 subunit glycine receptors in inflammatory pain. Front Mol Neurosci 2:14

Haverkamp S, Müller U, Harvey K et al (2003) Diversity of glycine receptors in the mouse retina: localization of the alpha3 subunit. J Comp Neurol 465:524–539

Hruskova B, Trojanova J, Kulik A, Kralikova M, Pysanenko K, Bures Z, Syka J, Trussell LO, Turecek R (2012) Differential distribution of glycine receptor subtypes at the rat calyx of held synapse. J Neurosci 32:17012–17024

Huang H, Trussell LO (2008) Control of presynaptic function by a persistent Na(+) current. Neuron 60:975–979

Hussy N, Deleuze C, Pantaloni A, Desarménien MG, Moos F (1997) Agonist action of taurine on glycine receptors in rat supraoptic magnocellular neurones: possible role in osmoregulation. J Physiol 502(3):609–621

Ichikawa H, Schulz S, Höllt V, Sugimoto T (2003) The somatostatin SST2A receptor in the rat trigeminal ganglion. Neuroscience 120:807–813

Javdani F, Holló K, Hegedűs K, Kis G, Hegyi Z, Dócs K, Kasugai Y, Fukazawa Y, Shigemoto R, Antal M (2015) Differential expression patterns of K(+)/Cl(−) cotransporter 2 in neurons within the superficial spinal dorsal horn of rats. J Comp Neurol. doi:10.1002/cne.23774

Kim Y, Trussell LO (2009) Negative shift in the glycine reversal potential mediated by a Ca^{2+}- and pH-dependent mechanism in interneurons. J Neurosci 29:11495–11510

Kirsch J, Betz H (1998) Glycine-receptor activation is required for receptor clustering in spinal neurons. Nature 392:717–720

Kneussel M, Brandstatter JH, Laube B, Stahl S, Muller U, Betz H (1999) Loss of Postsynaptic GABAA Receptor Clustering in Gephyrin-Deficient Mice. J Neurosci 19:9289–9297

Kopp-Scheinpflug C, Dehmel S, Tolnai S, Dietz B, Milenkovic I, Rübsamen R (2008) Glycine-mediated changes of onset reliability at a mammalian central synapse. Neuroscience 157:432–445

Kubota H, Alle H, Betz H, Geiger JRP (2010) Presynaptic glycine receptors on hippocampal mossy fibers. Biochem Biophys Res Commun 393:587–591

Labrakakis C, Tong C-K, Weissman T, Torsney C, MacDermott AB (2003) Localization and function of ATP and GABAA receptors expressed by nociceptors and other postnatal sensory neurons in rat. J Physiol 549:131–142

Legendre P (2001) The glycinergic inhibitory synapse. Cell Mol Life Sci 58:760–793

Legendre P (2002) Desensitization of homomeric alpha 1 glycine receptor increases with receptor density. Mol Pharmacol 62:817–827

Levi S, Vannier C, Triller A (1998) Strychnine-sensitive stabilization of postsynaptic glycine receptor clusters. J Cell Sci 111:335–345

Lorenzo L-E, Godin AG, Wang F, St-Louis M, Carbonetto S, Wiseman PW, Ribeiro-da-Silva A, De Koninck Y (2014) Gephyrin clusters are absent from small diameter primary afferent terminals despite the presence of GABA(A) receptors. J Neurosci 34:8300–8317

Lynch JW (2009) Native glycine receptor subtypes and their physiological roles. Neuropharmacology 56:303–309

Matsubara A, Laake JH, Davanger S, Usami S, Ottersen OP (1996) Organization of AMPA Receptor Subunits at a Glutamate synapse: a quantitative immunogold analysis of hair cell synapses in the rat organ of corti. J Neurosci 16:4457–4467

Mitchell K, Spike RC, Todd AJ (1993) An immunocytochemical study of glycine receptor and GABA in laminae I–III of rat spinal dorsal horn. J Neurosci 13:2371–2381

Mohammadi B, Krampfl K, Cetinkaya C, Moschref H, Grosskreutz J, Dengler R, Bufler J (2003) Kinetic analysis of recombinant

mammalian α1 and α1β glycine receptor channels. Eur Biophys J 32:529–536

Moon YS, Paik SK, Seo JH, Yi HW, Cho YS, Moritani M, Yoshida A, Ahn DK, Kim YS, Bae YC (2008) GABA- and glycine-like immunoreactivity in axonal endings presynaptic to the vibrissa afferents in the cat trigeminal interpolar nucleus. Neuroscience 152:138–145

Muller E, Le-Corronc H, Legendre P (2008) Extrasynaptic and postsynaptic receptors in glycinergic and GABAergic neurotransmission: a division of labor? Front Mol Neurosci 1:3

Ottersen OP, Storm-Mathisen J, Madsen S, Skumlien S, Strømhaug J (1986) Evaluation of the immunocytochemical method for amino acids. Med Biol 64:147–158

Paik SK, Bae JY, Park SE, Moritani M, Yoshida A, Yeo EJ, Choi KS, Ahn DK, Moon C, Shigenaga Y, Bae YC (2007) Developmental changes in distribution of γ-aminobutyric acid- and glycine-immunoreactive boutons on rat trigeminal motoneurons. I. Jaw-closing motoneurons. J Comp Neurol 503:779–789

Paik SK, Lee HJ, Choi MK, Cho YS, Park MJ, Moritani M, Yoshida A, Kim YS, Bae YC (2009) Ultrastructural analysis of glutamate-, GABA-, and glycine-immunopositive boutons from supratrigeminal premotoneurons in the rat trigeminal motor nucleus. J Neurosci Res 87:1115–1122

Paik SK, Park SK, Jin JK, Bae JY, Choi SJ, Yoshida A, Ahn DK, Bae YC (2011) Ultrastructural analysis of glutamate-immunopositive synapses onto the rat jaw-closing motoneurons during postnatal development. J Neurosci Res 89:153–161

Paik SK, Kwak WK, Bae JY, Na YK, Park SY, Yi HW, Ahn DK, Ottersen OP, Yoshida A, Bae YC (2012a) Development of γ-aminobutyric acid-, glycine-, and glutamate-immunopositive boutons on rat jaw-opening motoneurons. J Comp Neurol 520:1212–1226

Paik SK, Kwak MK, Bae JY, Yi HW, Yoshida A, Ahn DK, Bae YC (2012b) γ-Aminobutyric acid-, glycine-, and glutamate-immunopositive boutons on mesencephalic trigeminal neurons that innervate jaw-closing muscle spindles in the rat: ultrastructure and development. J Comp Neurol 520:3414–3427

Price GD, Trussell LO (2006) Estimate of the chloride concentration in a central glutamatergic terminal: a gramicidin perforated-patch study on the calyx of held. J Neurosci 26:11432–11436

Ribeiro-da-Silva A, Coimbra A (1982) Two types of synaptic glomeruli and their distribution in laminae I-III of the rat spinal cord. J Comp Neurol 209:176–186

Sassoe-Pognetto M, Wassle H, Grunert U (1994) Glycinergic synapses in the rod pathway of the rat retina: cone bipolar cells express the alpha 1 subunit of the glycine receptor. J Neurosci 14:5131–5146

Shigenaga Y, Yoshida A, Tsuru K, Mitsuhiro Y, Otani K, Cao CQ (1988) Physiological and morphological characteristics of cat masticatory motoneurons—intracellular injection of HRP. Brain Res 461:238–256

Shigenaga Y, Moritani M, Oh SJ, Park KP, Paik SK, Bae JY, Kim HN, Ma SK, Park CW, Yoshida A, Ottersen OP, Bae YC (2005) The distribution of inhibitory and excitatory synapses on single, reconstructed jaw-opening motoneurons in the cat. Neuroscience 133:507–518

Singer JH, Berger AJ (2000) Development of inhibitory synaptic transmission to motoneurons. Brain Res Bull 53:553–560

Storm-Mathisen J, Leknes AK, Bore AT, Vaaland JL, Edminson P, Haug F-MŠ, Ottersen OP (1983) First visualization of glutamate

and GABA in neurones by immunocytochemistry. Nature 301:517–520

Sugimoto T, Fujiyoshi Y, He Y-F, Xiao C, Ichikawa H (1997a) Trigeminal primary projection to the rat brainstem sensory trigeminal nuclear complex and surrounding structures revealed by anterograde transport of cholera toxin B subunit-conjugated and Bandeiraea simplicifolia isolectin B4-conjugated horseradish peroxidase. Neurosci Res 28:361–371

Sugimoto T, Fujiyoshi Y, Xiao C, He YF, Ichikawa H (1997b) Central projection of calcitonin gene-related peptide (CGRP)- and substance P (SP)-immunoreactive trigeminal primary neurons in the rat. J Comp Neurol 378:425–442

Takahashi T, Momiyama A, Hirai K, Hishinuma F, Akagi H (1992) Functional correlation of fetal and adult forms of glycine receptors with developmental changes in inhibitory synaptic receptor channels. Neuron 9:1155–1161

Takumi Y, Ramírez-León V, Laake P, Rinvik E, Ottersen OP (1999) Different modes of expression of AMPA and NMDA receptors in hippocampal synapses. Nat Neurosci 2:618–624

Todd AJ, Spike RC, Chong D, Neilson M (1995) The Relationship Between Glycine and Gephyrin in Synapses of the Rat Spinal Cord. Eur J Neurosci 7:1–11

Todd AJ, Watt C, Spike RC, Sieghart W (1996) Colocalization of GABA, glycine, and their receptors at synapses in the rat spinal cord. J Neurosci 16:974–982

Triner JC (2013) Defining neurochemical properties and functions of primary sensory neurons in the rat trigeminal ganglion, Dissertation, University of Plymouth

Trojanova J, Kulik A, Janacek J, Kralikova M, Syka J, Turecek R (2014) Distribution of glycine receptors on the surface of the mature calyx of Held nerve terminal. Front Neural Circuits 8:120

Turecek R, Trussell LO (2001) Presynaptic glycine receptors enhance transmitter release at a mammalian central synapse. Nature 411:587–590

Turecek R, Trussell LO (2002) Reciprocal developmental regulation of presynaptic ionotropic receptors. Proc Natl Acad Sci USA 99:13884–13889

Watson AHD (2004) Synaptic interactions between the terminals of slow-adapting type II mechanoreceptor afferents and neurones expressing gamma-aminobutyric acid- and glycine-like immunoreactivity in the rat spinal cord. J Comp Neurol 471:168–179

Witschi R, Punnakkal P, Paul J, Walczak J-S, Cervero F, Fritschy J-M, Kuner R, Keist R, Rudolph U, Zeilhofer HU (2011) Presynaptic alpha2-GABAA receptors in primary afferent depolarization and spinal pain control. J Neurosci 31:8134–8142

Wotherspoon G, Priestley JV (1999) Expression of the 5-HT1B receptor by subtypes of rat trigeminal ganglion cells. Neuroscience 95:465–471

Xiong W, Cui T, Cheng K, Yang F, Chen S-R, Willenbring D, Guan Y, Pan H-L, Ren K, Xu Y, Zhang L (2012) Cannabinoids suppress inflammatory and neuropathic pain by targeting α3 glycine receptors. J Exp Med 209:1121–1134

Xiong W, Chen S-R, He L, Cheng K, Zhao Y-L, Chen H, Li D-P, Homanics GE, Peever J, Rice KC, Wu L, Pan H-L, Zhang L (2014) Presynaptic glycine receptors as a potential therapeutic target for hyperekplexia disease. Nat Neurosci 17:232–239

Zhang N, Ottersen OP (1992) Differential cellular distribution of two sulphur-containing amino acids in rat cerebellum. Exp Brain Res 90:11–20